REPROGRAMMABLE, DIGITAL BEAM STEERING GPS RECEIVER TECHNOLOGY FOR ENHANCED SPACE VEHICLE OPERATIONS

Randy Silva, Rhip Worrell, and Alison Brown NAVSYS Corporation

ABSTRACT

Spaceborne GPS technology is being widely accepted by both the commercial space industry and by NASA as the key enabler for improving space operations. GPS applications include: autonomous orbit operations, accurate positioning and time synchronization, attitude determination and accurate relative ranging between vehicles for formation flying. The use of GPS for space missions will improve space vehicle autonomy, and reduce design and operations cost through the infusion of GPS technology. In this paper the design of the digital beam steering receiver is described and test results are presented showing its performance advantages for future space vehicle operations.

INTRODUCTION

NAVSYS has developed a next generation digital GPS receiver that can provide enhanced navigation and guidance performance for space applications through the use of a digital beam steering antenna array. This has the following advantages for space applications.

- All-around satellite visibility using multiple antenna elements to maximize navigation continuity for rotating space vehicles
- Gain from beam steering enables low signal strength satellites to be tracked allowing operation at high orbit altitudes
- Beam steering reduces the effect of multipath on the GPS signals improving the navigation and attitude accuracy.
- Software reprogrammable architecture allows the receiver to be reconfigured and optimized for operation in different phases of flight.

The principle of operation of the software reprogrammable digital beam steering receiver is described in this paper and test data is presented demonstrating the benefits that can be accrued for space missions using this receiver design.

HIGH GAIN ADVANCED GPS RECEIVER

NAVSYS' High-gain Advanced GPS Receiver (HAGR)[1] is a software reprogrammable, digital beam steering GPS receiver. The HAGR components are illustrated in Figure 1. With the HAGR digital beam steering implementation, each antenna RF input is converted to a digital signal using a Digital Front-End (DFE). The HAGR can be configured to operate with up to 16 antenna elements (L1 and L2) with the antenna elements installed in any user specified antenna array pattern.

Each DFE board in the HAGR can convert signals from eight antenna elements. The digital signals from the set of the antenna inputs are then provided to the HAGR digital signal processing cards. The HAGR can be configured to track up to 12 satellites providing L1 C/A and L1 and L2 P(Y) observations when operating in the keyed mode. The digital signal processing is performed in firmware, downloaded from the host computer. Since the digital spatial processing is unique for each satellite channel, the weights can be optimized for the particular satellites being tracked. The digital architecture allows the weights to be computed in the HAGR software and then downloaded to be applied pre-correlation to create a digital adaptive antenna pattern to optimize the signal tracking performance.

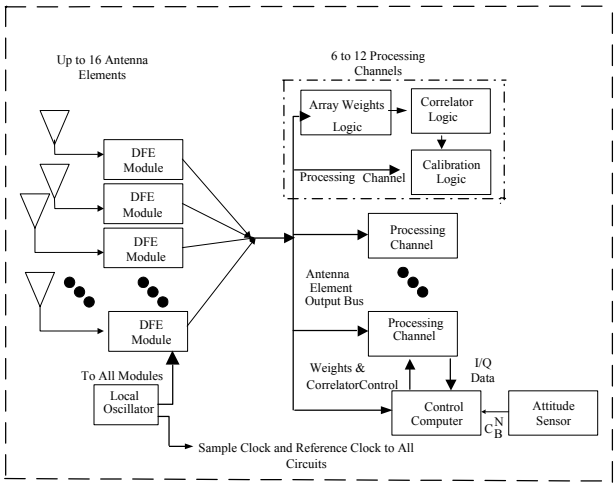

Figure 1 P(Y) HAGR System Block Diagram

DIGITAL BEAM STEERING

The digital signal from each of the HAGR antenna elements can be described by the following equation.

$$y_k(t) = \sum_{i=1}^{Ns} s_i(\underline{x}_k, t) + n_k(t) + \sum_{k=1}^{Nj} j_j(\underline{x}_k, t)$$

where $s_i(\underline{x}_k,t)$ is the ith GPS satellite signal received at the kth antenna element

$n_k(t)$ is the noise introduced by the kth DFE

$j_j(\underline{x}_l,t)$ is the filtered jth jammer signal received at the kth antenna element

The GPS satellite signal at each antenna element ($\underline{x}_k$) can be calculated from the following equation.

$$s_i(\underline{x}_k, t) = s_i(0,t)\exp\{-i\frac{2\pi}{\lambda}\underline{1}_i^T \underline{x}_k) = s_i(0,t)e_{sik}$$

where $s_i(0,t)$ is the satellite signal at the array center and

$\underline{1}_i$ is the line-of-sight to that satellite

e_{sik} are the elements of a vector of phase angle offsets for satellite i to each element k

The combined digital array signal, z(t), is generated from summing the weighted individual filtered DFE signals. This can be expressed as the following equation.

$$z(t) = \underline{w}' \underline{y}(t) = \underline{w}'\left[\sum_{i=1}^{Ns} s_i(t)\underline{e}_{si} + \underline{n}(t) + \sum_{l=1}^{Nj} j_j(t)\underline{e}_{jl}\right]$$

With beam steering, the optimal weights are selected to maximize the signal/noise ratio to the particular satellite being tracked. These are computed from the satellite phase angle offsets as shown in the following equation.

$$\underline{w}_{BS} = \begin{bmatrix} \exp\{-i\frac{2\pi}{\lambda}\underline{1}_i^T \underline{x}_1)\\ \dot{} \\ \exp\{-i\frac{2\pi}{\lambda}\underline{1}_i^T \underline{x}_M)\end{bmatrix} = \underline{e}_s$$

In Figure 2 and Figure 3 the antenna patterns created by the digital antenna array are shown for four of the satellites tracked. The HAGR can track up to 12 satellites simultaneously. The antenna pattern provides the peak in the direction of the satellite tracked (marked 'x' in each figure). The beams follow the satellites as they move across the sky. Since the L2 wavelength is larger than the L1 wavelength, the antenna beam width is wider for the L2 antenna pattern than for the L1.

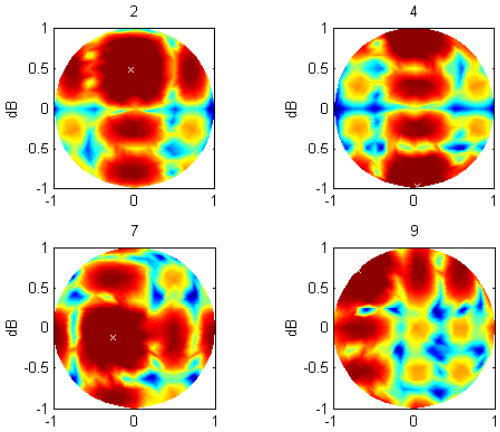

Figure 2 L1 Antenna Pattern

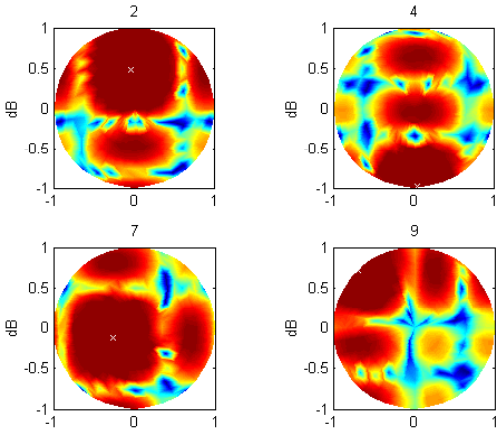

Figure 3 L2 Antenna Pattern

ALL-AROUND SATELLITE VISIBILITY

The purpose of this testing was to demonstrate the ability of the HAGR to form a composite signal from antennas located in a non-planar configuration.

This testing was performed to show the capability of the HAGR to provide all-around satellite visibility using multiple antenna elements. The test configuration is shown in Figure 4 and a picture of the test fixture is shown in Figure 5.

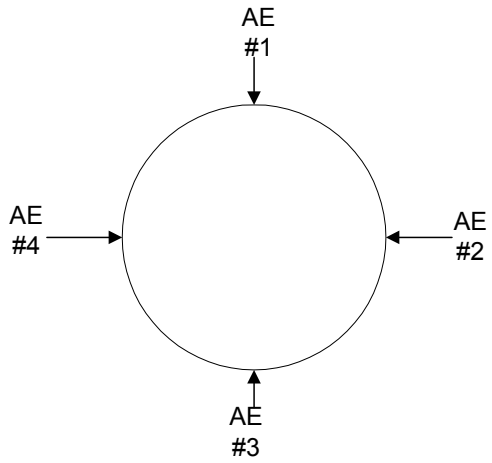

Figure 4 Four-Element All-around Visibility Antenna Testing

Figure 5 Satellite Test Fixture

In Figure 6, a sky plot is shown with the locations of the GPS satellites tracked during the test. In Figure 7, the satellite PRNs that were tracked during the test are plotted against time, and in Table 1, the signal-to-noise ratios of the satellites tracked during the test are listed. From this test data, it is evident that the 3-D beam forming is functioning correctly. All of the satellites above the horizon were tracked with the exception of satellites 8 and 10, which were not selected by the 8-channel GPS receiver. The signal-to-noise ratio is also comparable with normal GPS operation indicating no noticeable degradation from the 4π steridian signal combining.

Table 1 All-around Satellite Visibility Test Data Summary

PRN	AZ	EL	C/N0
1	155	23	42
2	245	19	44
3	55	31	48
7	205	13	39
8	305	13	-
10	311	10	-
11	125	10	37
13	294	51	45
15	98	12	43
18	189	60	47
19	341	72	44
27	305	45	46
31	100	53	47

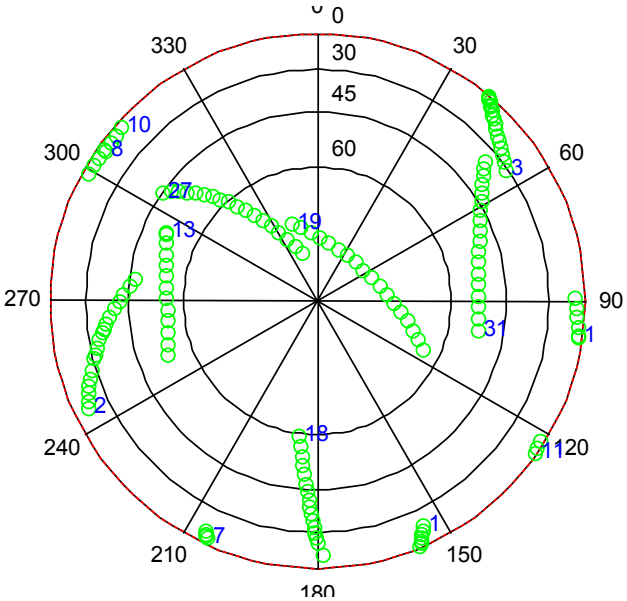

Figure 6 Skyplot of 3-D Beam steering Satellite Visibility

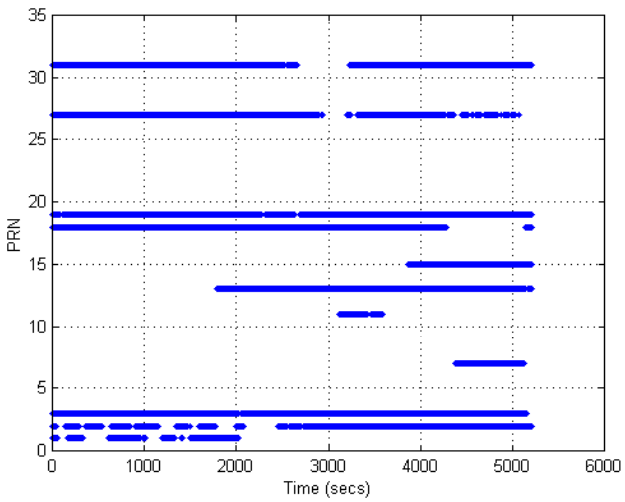

Figure 7 All-around Visibility Tests - SVs tracked

HIGH GAIN SATELLITE TRACKING

The directivity of the digital beam-forming provides gain in the direction of the GPS satellites. This improves the ability of the digital beam steering receiver to be able to track GPS satellites with low signal power, for example, from a space platform located above the GPS satellite constellation. With a 16 element array, the beam steering provides up to 12 dB of additional gain. With a 7 element array, up to 8.45 dB of additional gain is provided. A data set was collected to observe the signal-to-noise ratio on the C/A and P(Y) code HAGR data over a period of 12 hours. From this data (Figure 8 and Figure 9), it can be seen that the beam steering increases the GPS signal strength to a value of 56 dB-Hz on the C/A code. As expected the P(Y) code observed signal strength is 3 dB lower.

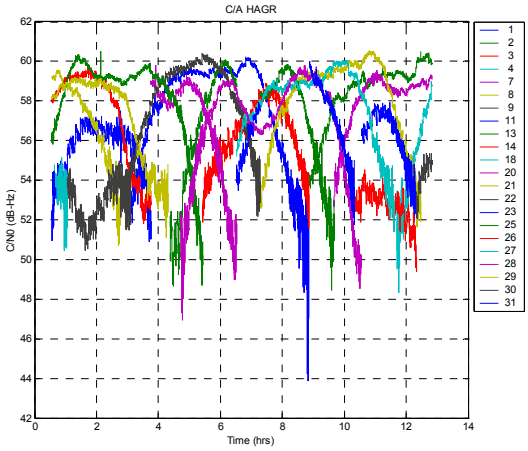

Figure 8 C/A HAGR Signal-to-Noise (dB-Hz)

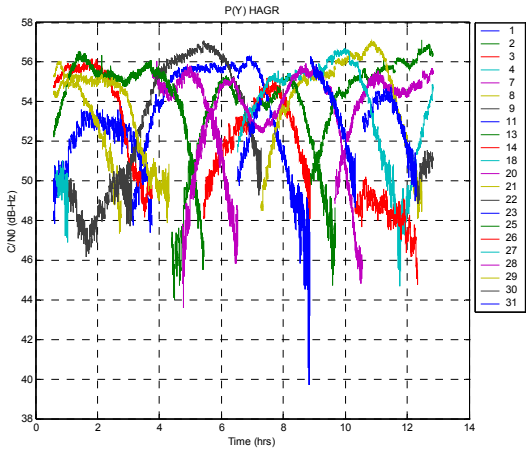

Figure 9 P(Y) HAGR Signal-to-Noise (dB-Hz)

MEASUREMENT NOISE AND MULTIPATH ERROR REDUCTION

The digital beam steering also improves the measurement accuracy and decreases the effect of multipath errors from signal reflections received from the spacecraft structure (e.g. solar panels or antenna arrays).

The GPS L1 pseudo-range and carrier-phase observations are described by the following equations.

$$PR_{i1}(m) = R_i + b_u + I_i + \Delta_{Ti} + \tau_{M1i} + n_{PR1}$$

$$CPH_{i1}(m) = N_1\lambda_1 + n_{CPH1} - (R_i + b_u - I_i + \Delta_{Ti} + \lambda_1\theta_{M1i})$$

The following errors affect the pseudo-range and carrier phase observations.

1. Ionosphere errors– (I)
2. Troposphere errors – these are the same on all of the observations (Δ_{Ti})
3. Receiver Measurement Noise – these are different on each of the observations (n_{PR1} , n_{CPH1})
4. Multipath Noise – these are different on each of the observations (τ_{M1i} , $\lambda_1\theta_{M1i}$)
5. Satellite and Station Position error - these affect the ability to correct for the Range to the satellite (R_i)
6. Receiver clock offset (bu)

From this equation, the L1 pseudo-range + carrier phase sum cancels out the common errors and the range to the satellite and observes the pseudo-range

and multipath errors as well as the change in the ionospheric offset.

$$PR_{i1} + CPH_{i1}(m) = 2I_i + \tau_{M1i} + n_{PR1} + N_1\lambda_1 + n_{CPH1} - \lambda_1\theta_{M1i}$$
$$= C + 2I_i + \tau_{M1i} + n_{PR1} + (n_{CPH1} - \lambda_1\theta_{M1i})$$
$$\approx C + 2I_i + \tau_{M1i} + n_{PR1}$$

The PR+CPH is plotted in Figure 11 for SV 25 and each of the receiver data sets. The short term (<100 sec) white receiver noise was removed by passing the PR+CPH observation through a linear filter. The drift caused by the ionosphere on each observation was removed using a polynomial estimator. The remaining cyclic error is an estimate of the multipath pseudo-range errors. The RMS white noise on the pseudo-range observations was computed by differencing the PR+CPH measurement. This is shown in Figure 12 and Figure 13 for all of the satellites tracked for the C/A and P(Y) code observations. The observed PR noise shows good correspondence with the predicted values, based on analysis of the tracking loops, shown in Figure 14. For C/N0 values above 52 dB-Hz, the P(Y) code HAGR provided pseudo-range accuracies of 5 cm (1-sigma) while for C/N0 values above 55 dB-Hz the C/A code observations were accurate to 15 cm. These values are for 1-Hz observations without any carrier smoothing applied. The mean observed RMS accuracies are summarized below in Table 2 with the average peak multipath PR errors observed.

The short term cyclic variations shown in Figure 11 are caused by multipath errors. The peak-to-peak cyclic PR variation for each of the receiver data sets was calculated to estimate the errors observed for each satellite from the pseudo-range multipath[1]. These errors are listed in Table 2 for each of the satellites. The HAGR spatial signal processing can also be used to detect the presence of multipath and adapt the antenna pattern to further minimize these errors.[[2,3] In Figure 10 spatial information from a 7-element phased array is shown that identifies the source of a strong multipath signal through direction of arrival (DOA) estimation using the MUSIC algorithm[4]. Testing has shown that the digital beam steering and spatial processing significantly reduces the multipath errors on the carrier phase observations. This is important for space applications which rely on the GPS carrier phase information, such as interferometric attitude determination.

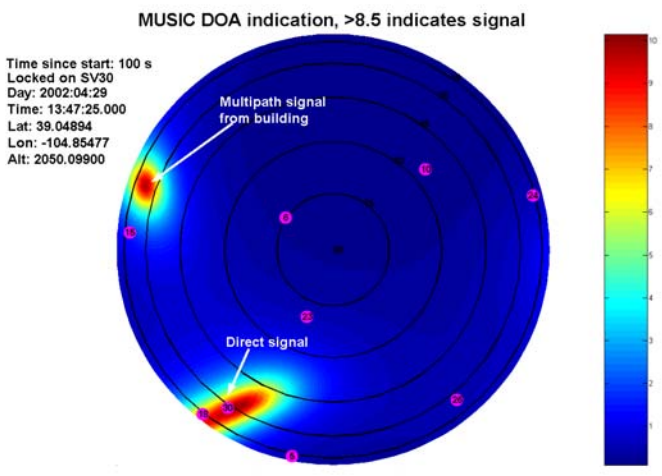

Figure 10 MUSIC direction of arrival estimation

Table 2 Mean PR Noise and M-path Peak Errors (m) (16-element array)

SVID	C/A HAGR RMS PR	C/A Mean Mpath PR	P(Y) HAGR RMS PR	P(Y) Mean Mpath PR
1	0.239	0.259	0.054	0.202
3	0.284	0.494	0.056	0.337
8	0.200	0.278	0.045	0.202
11	0.278	0.535	0.059	0.287
13	0.252	0.321	0.059	0.260
14	0.214	0.359	0.049	0.350
20	0.222	0.267	0.050	0.164
21	0.252	0.261	0.058	0.133
22	0.248	0.318	0.047	0.217
25	0.202	0.362	0.044	0.265
27	0.183	0.270	0.044	0.178
28	0.236	0.366	0.055	0.272
29	0.225	0.312	0.050	0.217
30	0.477	0.791	0.089	0.624
31	0.325	0.266	0.055	0.135

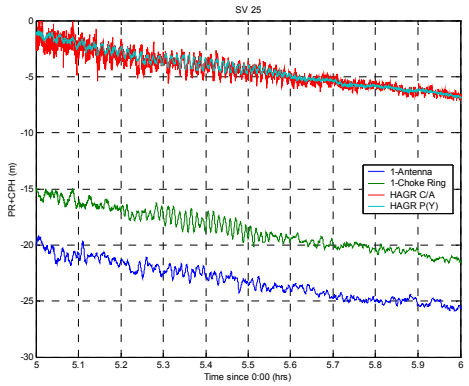

Figure 11 PR+CPH (m) - SV 25

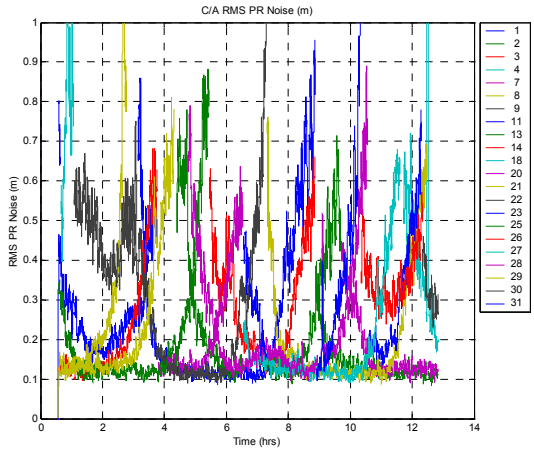

Figure 12 HAGR C/A Code Pseudo-Range Noise (m) (16-element array– no carrier smothing)

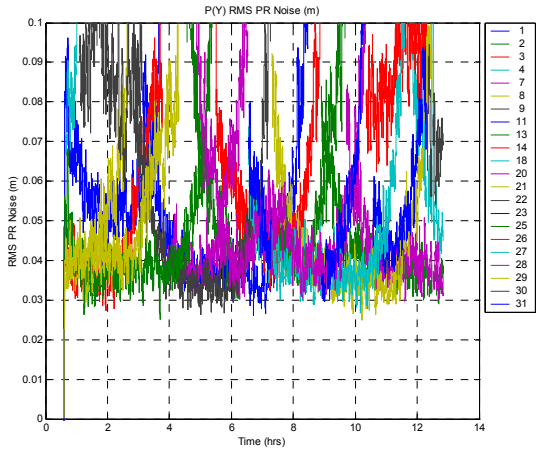

Figure 13 HAGR P(Y) Code Pseudo-Range Noise (m) (16-element array– no carrier smothing)

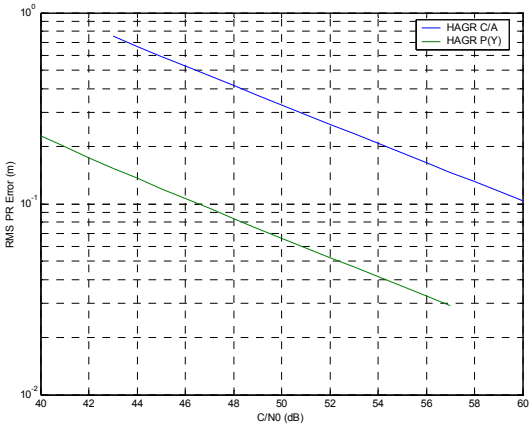

Figure 14 C/A and P(Y) HAGR RMS PR error versus C/N0

SOFTWARE REPROGRAMMABLE GPS RECEIVER

The flexible Software GPS Receiver (SGR) architecture leveraged by the HAGR allows the GPS signal processing software and firmware to be easily ported to run on space qualified signal processing and host computer cards.[5] The GPS software radio architecture adopted by the HAGR shown in Figure 15 allows the receiver configuration to be optimized depending on the phase of flight[5]. For example, different antenna inputs and navigation modes could be used during launch and orbit entry than during the remaining mission life where the receiver could be optimized for autonomous orbit estimation and stationkeeping.

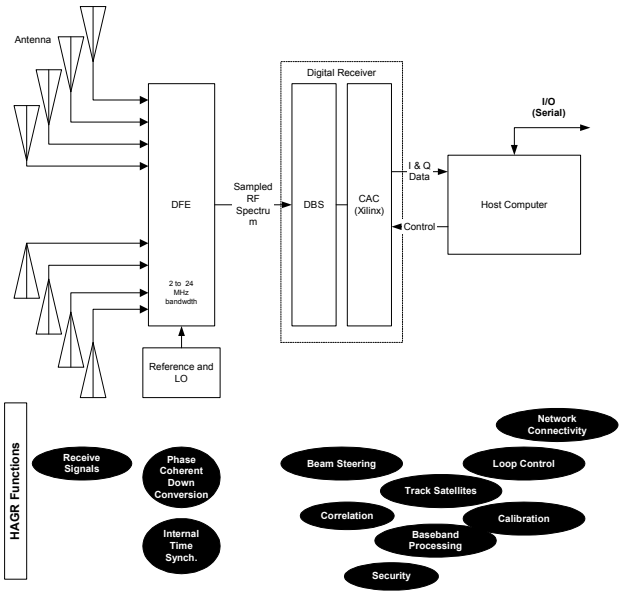

Figure 15 NAVSYS Software GPS Receiver Architecture

CONCLUSION

The test data presented in this paper has shown that the digital beam steering architecture has advantages in: increasing the received GPS signal/noise ratio, which improves the tracking performance for low power satellite signals; improving the measurement accuracy for precision applications such as rendezvous, docking or formation flying; minimizing carrier phase multipath errors which can result in improved interferometric attitude determination.

NAVSYS is currently developing a design for a space-borne version of our reprogrammable, digital beam steering GPS receiver product under contract to AFRL/VS and NASA Goddard Space Flight

Center. This modular, flexible architecture is designed to be ported from our in-house test-bed to a variety of space-qualified signal processing boards and host computers to provide an embedded GPS capability. The design also allows the receiver to be reconfigured in-flight to optimize the GPS tracking performance depending on the needs of each phase of the mission.

ACKNOWLEDGEMENTS

This work is being sponsored under an SBIR contract to AFRL/VS and to NASA GSFC. The authors would like to express their appreciation for the support of these organizations in the development of this new technology.

BIOGRAPHIES

Randy Silva is a Senior Scientist at NAVSYS Corporation where his work includes simulation, design, implementation, and testing of real-time GPS/Inertial systems. He holds a B.A. in Computer Science from the University of Colorado.

Rhip Worrell is the Chief Operating Officer of NAVSYS Corporation. He manages where he is responsible for all Administrative and Technical Operations (Engineering, Project Control, and Production). He has a M.S. in Aerospace Engineering from the University of Colorado and a B.S. in Astronautical Engineering from USAF Academy.

Alison Brown is the President and CEO of NAVSYS Corporation. She has a PhD in Mechanics, Aerospace, and Nuclear Engineering from UCLA, an MS in Aeronautics and Astronautics from MIT, and an MA in Engineering from Cambridge University. In 1986, she founded NAVSYS Corporation. Currently she is a member of the GPS-III Independent Review Team and Scientific Advisory Board for the USAF and serves on the GPS World editorial advisory board.

REFERENCES

1 A. Brown, N. Gerein, "Test Results from a Digital P(Y) Code Beamsteering Receiver for Multipath Minimization," ION 57th Annual Meeting, Albuquerque, NM, June 2001.

2 A. Brown, “Performance and Jamming Test Results of a Digital Beamforming GPS Receiver,” Joint Navigation Conference, Orlando, FL, May, 2002.

3 D. Sullivan, R. Silva, and A. Brown, “High Accuracy Differential and Kinematic GPS Positioning using a Digital Beam Steering Receiver,” Proceedings of 2002 Core Technologies for Space Systems Conference, Colorado Springs, CO, November 2002.

4 A. Brown and K. Stolk; “Rapid Ambiguity Resolution using Multipath Spatial Processing for High Accuracy Carrier Phase, Proceedings of ION GPS 2002, Portland, OR, September 2002.

5 N. Gerein, A. Brown, “Modular GPS Software Radio Architecture,” Proceedings of ION GPS 2001, Salt Lake City, Utah, September 2001.